



Supplement of

Debris flow event on Osorno volcano, Chile, during summer 2017: new interpretations for chain processes in the southern Andes

Ivo Janos Fustos-Toribio et al.

Correspondence to: Marcelo Somos-Valenzuela (marcelo.somos@ufrontera.cl) and Ivo Janos Fustos-Toribio (ivo.fustos@ufrontera.cl)

The copyright of individual parts of the supplement might differ from the article licence.

1 Data

The calibrated parameters with the high sensitivity correspond to the basal friction angle, fluid friction coefficient, and environmental drag coefficient. We considered a solid-phase density of 2.8 (g/cm³) due to the Osorno volcano has a basalt-andesite composition.

Symbol	Parameter	Value	units	Source/reference
ρ_s	Solid material density	2800	kg/m ³	Oyarzun (2019) and Somos-Valenzuela et al., 2020
ρ_f	Fluid material density	1000	kg/m ³	Standard for water
ϕ	Internal friction angle *	32.4	Degree	This study, laboratory measurements of in-situ sample
δ	Basal friction angle	6	Degree	Mergili et al. 2018a
C	Virtual mass	0.5	-	Mergili et al. 2017
U_T	Terminal velocity	1	m/s	Mergili et al. 2017
P	Parameter for combination of solid- and fluid-like contributions to drag resistance	0.5	-	Mergili et al. 2018a
Re_p	Particle Reynolds number	1	-	Mergili et al. 2017 and Oyarzun 2019
J	Exponent for drag	1	-	Mergili et al.

				2017 and Oyarzun (2019)
N_R	Quasi-Reynolds number	4,5	-	Oyarzun (2019)
N_{RA}	Mobility number	3	-	Oyarzun (2019) and Somos- Valenzuela et al. (2020)
α	Viscous shearing coefficient for fluid	0	-	Mergili et al. 2017
ξ	Solid concentration distribution with depth	0	-	Oyarzun (2019) and Somos- Valenzuela et al. (2020)
C_{AD}	Ambient drag coefficient	0,02	-	Zwinger et al. (2003)
C_E	Entrainment coefficient	-6,69	kg^{-1}	Oyarzun (2019) and Somos- Valenzuela et al. (2020)
C_{FF}	Fluid friction coefficient	0,001		Oyarzun (2019) and Mergili et al. 2020

Table S1. Model parameters used in r.avafow.

2 Methodology

Parameter	Value
Hydrogram	No
Diffusive control	Yes
Volume conservation	Yes
Surface control	Yes

Drag exponent	Linear
Step Save time (t)	10
Simulation lenght (s)	500
Flow stop	No
Name	Petrohue
DEM	ASTER or SRTM
Water content range	40% - 70%

Table S2. Model setup in r.avaflow

2.1 Model output

The main output results correspond to the flow height each 10 s of simulation, maximum height reached by the flow, pressure, topography variations, flow velocity and flow volume.

3 Additional results

3.1 Simulations

3.1.1 Simulation with SRTM

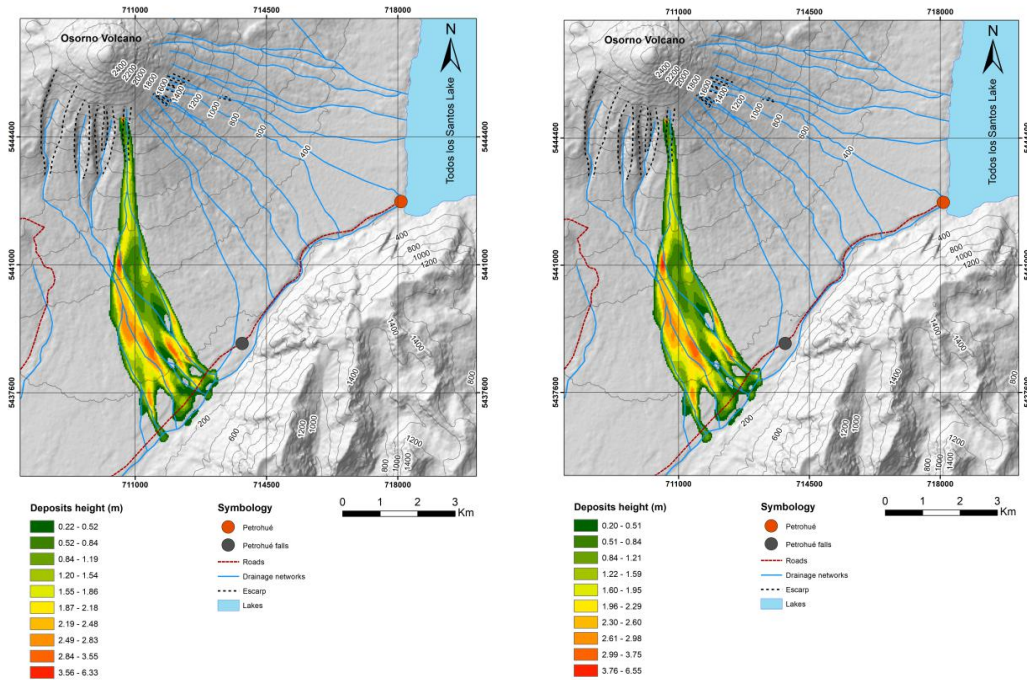


Figure S1. Left: Simulation with r.avaflow using 40% of initial water content. Right: Simulation with r.avaflow using 45% of initial water content.

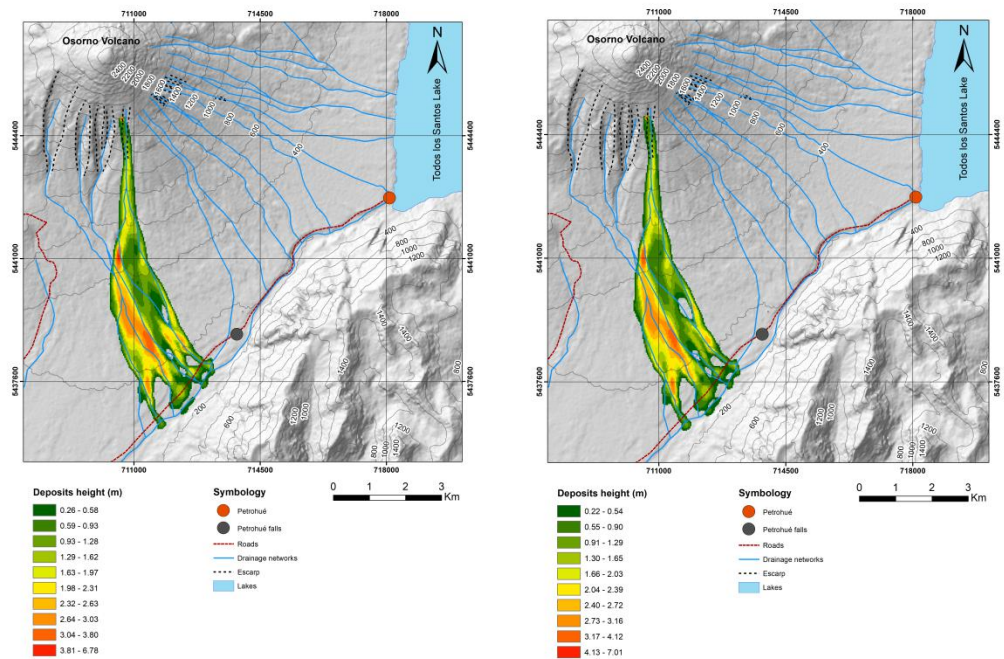


Figure S2. Left: Simulation with r.avaflow using 50% of initial water content. Right: Simulation with r.avaflow using 55% of initial water content.

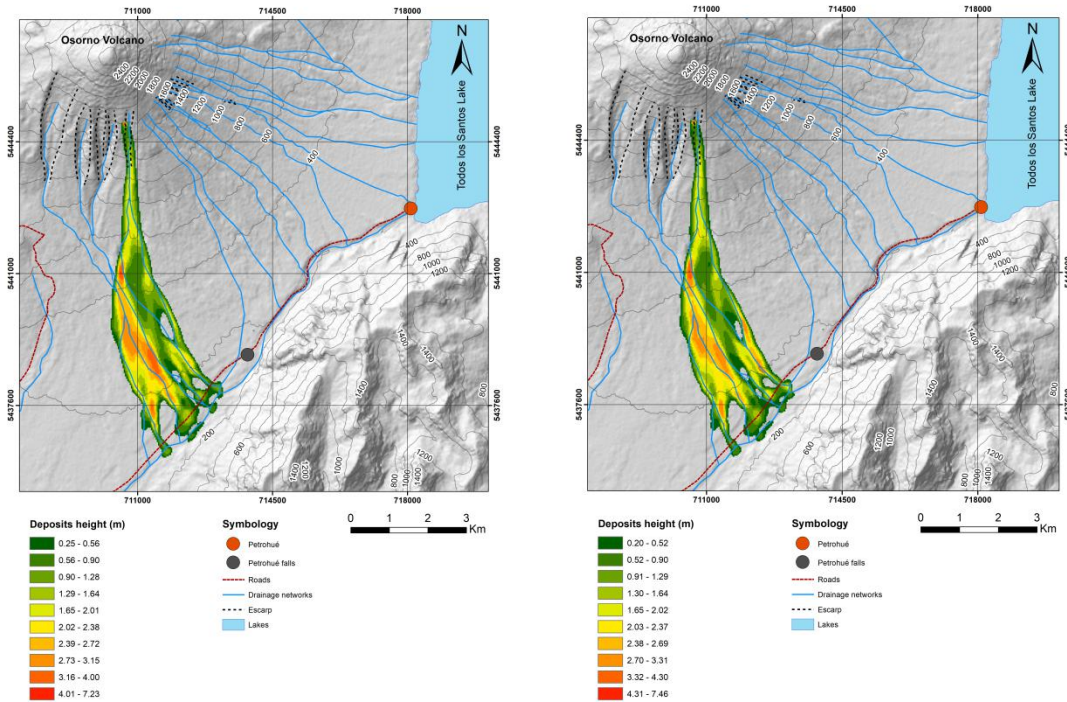


Figure S3. Left: Simulation with r.avaflow using 60% of initial water content. Right: Simulation with r.avaflow using 65% of initial water content.

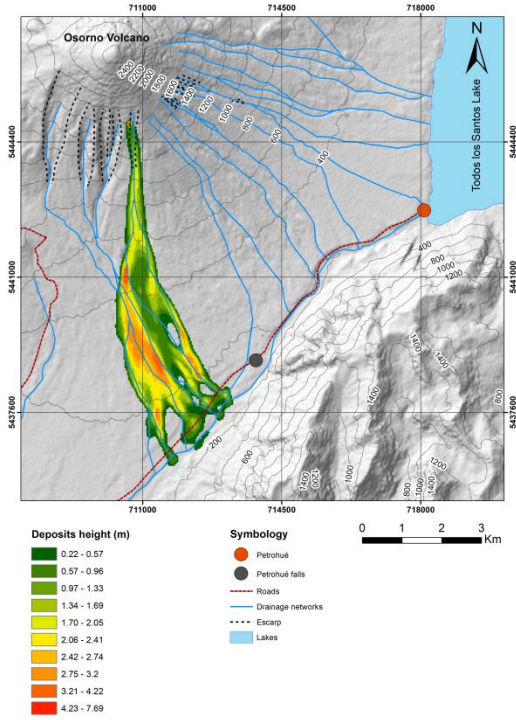


Figure S4. Left: Simulation with r.avaflow using 70% of initial water content.

3.1.2 Simulation with ASTER GDEM

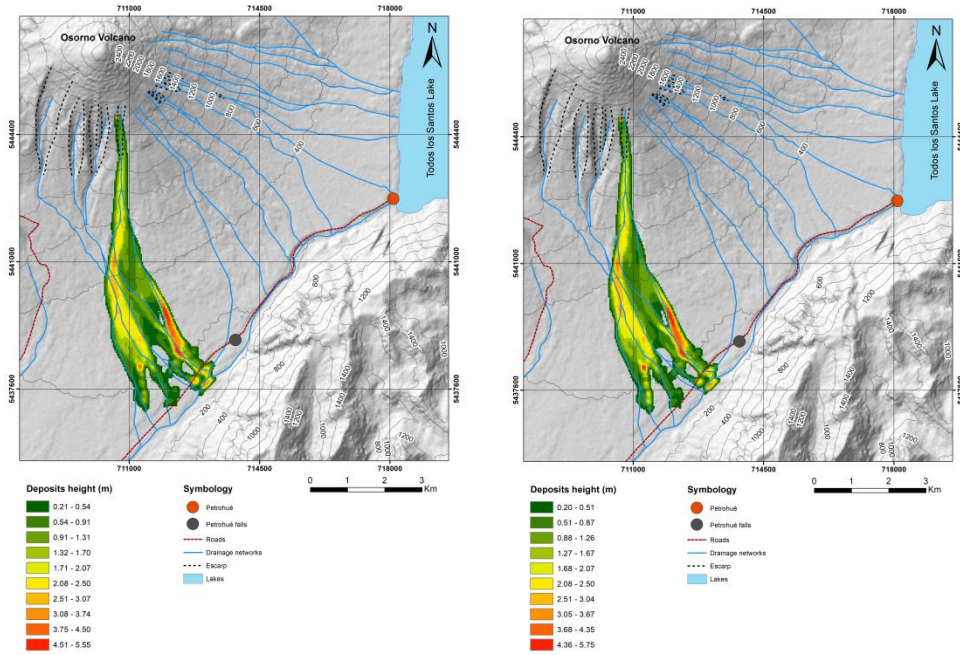


Figure S5. Left: Simulation with r.avaflow using 40% of initial water content. Right: Simulation with r.avaflow using 45% of initial water content.

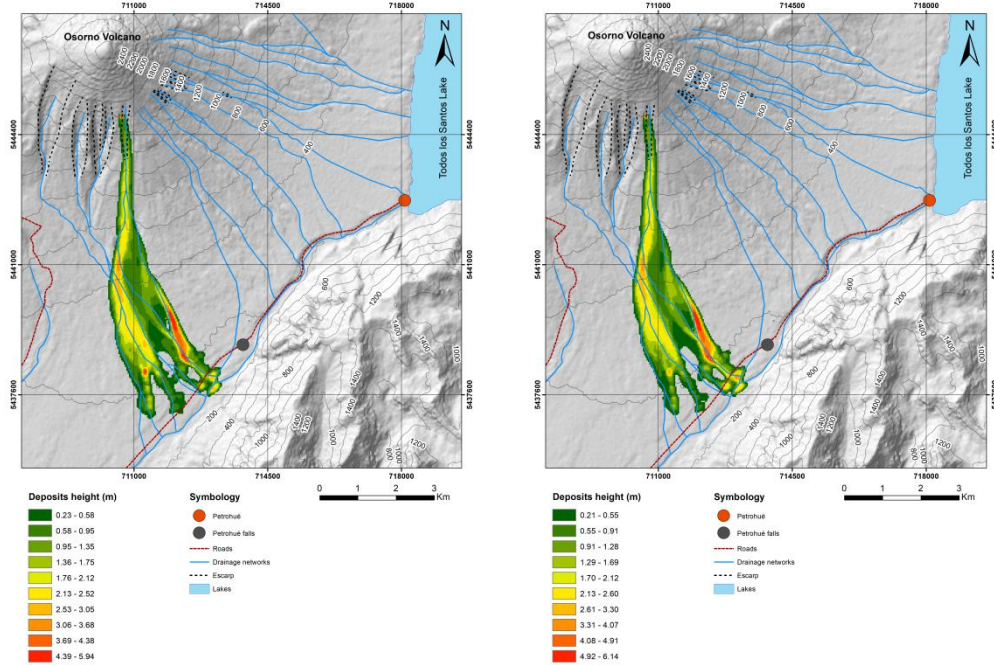


Figure S6. Left: Simulation with r.avaflow using 50% of initial water content. Right: Simulation with r.avaflow using 55% of initial water content.

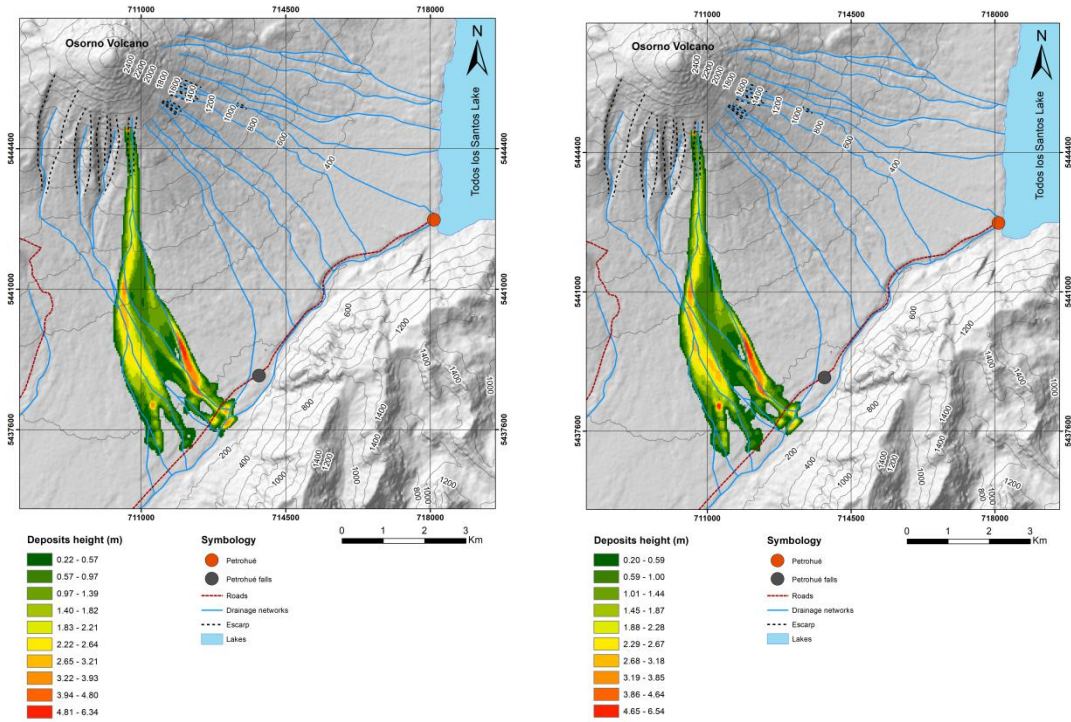


Figure S7. Left: Simulation with r.avaflow using 60% of initial water content. Right: Simulation with r.avaflow using 65% of initial water content.

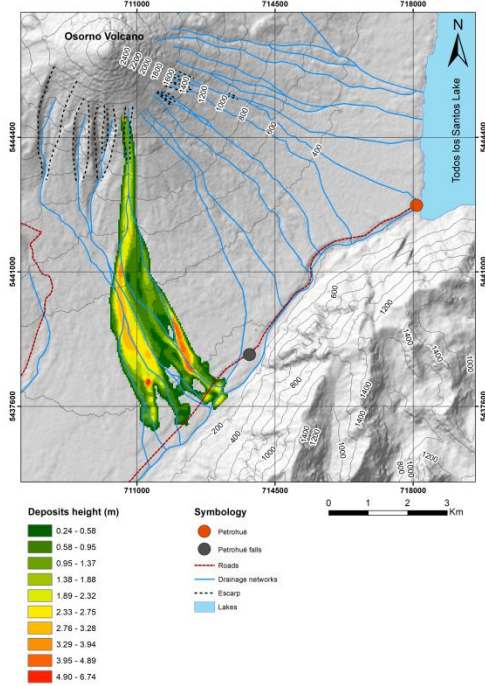


Figure S8. Simulation with r.avaflow using 70% of initial water content.

4 Summary

Simulation code	Initial water content (%)	Area (m^2)	Runout (km)	Max height (m)	Final height (m)	Initial volume of lava fall	Final volume
DEM ASTER GDEM							
Simulation 195	40%	7.699.909	8,06	5,55	1,63	16.670	468.172
Simulation 196	45%	7.752.633	8,06	5,75	1,10	16.670	464.564
Simulation 159	50%	7.656.355	8,05	5,94	1,74	16.670	475.812
Simulation 197	55%	7.533.716	8,04	6,14	1,62	16.670	485.413
Simulation 160	60%	7.631.139	8,08	6,34	2,13	16.670	499.523
Simulation 198	65%	7.797.333	8,08	6,54	1,13	16.670	499.363
Simulation 161	70%	7.827.133	8,05	6,74	1,58	16.670	517.670
DEM SRTM							
Simulation 95	40%	8.364.900	8,78	6,33	1,87	16.670	483.828
Simulation 96	45%	8.547.565	8,78	6,55	1,60	16.670	499.563

Simulation 43	50%	8.300.874	8,78	6,78	1,64	16.670	507.000
Simulation 97	55%	8.483.538	8,78	7,01	1,28	16.670	527.344
Simulation 44	60%	8.308.406	8,78	7,23	1,33	16.670	528.373
Simulation 98	65%	8.643.605	8,79	7,46	1,43	16.670	533.413
Simulation 45	70%	8.600.293	8,80	7,69	1,59	16.670	544.903

Figure S9. Results of r avaflow using ASTER and SRTM models.

N° Simulation	Error in runout (%)	Back-analysis height error (%)	Runout (km)	Back-analysis height (m)
DEM ASTER GDEM with respect to back-analysis height				
Simulation 195	-8%	63%		
Simulation 196	-8%	10%		
Simulation 159	-7%	16%		
Simulation 197	-8%	8%		
Simulation 160	-7%	42%		
Simulation 198	-7%	-25%		
Simulation 161	-7%	5%		
DEM SRTM with respect to back-analysis height				
Simulation 95	1%	25%		
Simulation 96	1%	7%		
Simulation 43	1%	9%		
Simulation 97	1%	-15%		
Simulation 44	1%	-11%		
Simulation 98	1%	-5%		
Simulation 45	1%	6%		

Figure S10. r avaflow error.

5 Reference

Mergili, M., Fischer, J. T., Krenn, J., & Pudasaini, S. P. (2017). r avaflow v1, an advanced open-source computational framework for the propagation and interaction of two-phase mass flows. Geoscientific Model Development, 10(2), 553-569.

Mergili, M., Frank, B., Fischer, J. T., Huggel, C., & Pudasaini, S. P. (2018). Computational experiments on the 1962 and 1970 landslide events at Huascarán (Peru) with r. avaflow: Lessons learned for predictive mass flow simulations. *Geomorphology*, 322, 15-28.

Mergili, M., Emmer, A., Juřicová, A., Cochachin, A., Fischer, J. T., Huggel, C., & Pudasaini, S. P. (2018b). How well can we simulate complex hydro-geomorphic process chains? The 2012 multi-lake outburst flood in the Santa Cruz Valley (Cordillera Blanca, Perú). *Earth surface processes and landforms*, 43(7), 1373-1389.

Mergili, M., Jaboyedoff, M., Pullarello, J., & Pudasaini, S. P. (2020). Back calculation of the 2017 Piz Cengalo–Bondo landslide cascade with r. avaflow: what we can do and what we can learn. *Natural Hazards & Earth System Sciences*, 20(2)

Oyarzún, J. (2019). Análisis de los factores gatillantes al flujo hiperconcentrado en Villa Santa Lucía y determinación de las condicionantes de un proceso futuro. Trabajo de Proyecto de Titulación para optar al Título de Ingeniero Civil. Universidad de La Frontera, Facultad de Ingeniería y ciencia.

Somos-Valenzuela, M. A., Oyarzún-Ulloa, J. E., Fustos-Toribio, I. J., Garrido-Urzua, N., & Chen, N. (2020). The mudflow disaster at Villa Santa Lucía in Chilean Patagonia: understandings and insights derived from numerical simulation and postevent field surveys. *Natural Hazards and Earth System Sciences*, 20(8), 2319–2333. <https://doi.org/10.5194/nhess-20-2319-2020>

Zwinger, T., Kluwick, A., & Sampl, P. (2003). Numerical simulation of dry-snow avalanche flow over natural terrain. In *Dynamic response of granular and porous materials under large and catastrophic deformations* (pp. 161-194). Springer, Berlin, Heidelberg.